

Signatures of Primordial Gravitational Waves on the Large-Scale Structure of the Universe

Pritha Bari^{1,2,*}, Angelo Ricciardone^{1,2,†}, Nicola Bartolo^{1,2,3,‡}, Daniele Bertacca^{1,2,3,§} and Sabino Matarrese^{1,2,3,4,||}

¹*Dipartimento di Fisica e Astronomia “G. Galilei,” Università degli Studi di Padova, via Marzolo 8, I-35131 Padova, Italy*

²*INFN, Sezione di Padova, via Marzolo 8, I-35131 Padova, Italy*

³*INAF—Osservatorio Astronomico di Padova, I-35122 Padova, Italy*

⁴*Gran Sasso Science Institute, I-67100 L’Aquila, Italy*

 (Received 3 December 2021; revised 22 June 2022; accepted 9 August 2022; published 26 August 2022)

We study the generation and evolution of second-order energy-density perturbations arising from primordial gravitational waves. Such “tensor-induced scalar modes” approximately evolve as standard linear matter perturbations and may leave observable signatures in the large-scale structure of the Universe. We study the imprint on the matter power spectrum of some primordial models which predict a large gravitational-wave signal at high frequencies. This novel mechanism, in principle, allows us to constrain or detect primordial gravitational waves by looking at specific features in the matter or galaxy power spectrum, thereby allowing us to probe them on a range of scales unexplored so far.

DOI: [10.1103/PhysRevLett.129.091301](https://doi.org/10.1103/PhysRevLett.129.091301)

Introduction.—Inflation in the early Universe [1] plays a crucial role in the standard model of cosmology, as it provides the seeds for structure formation through scalar (energy-density) perturbations originating from quantum vacuum oscillations of the scalar field driving the accelerated Universe expansion. At the same time, inflation produces tensor (gravitational-wave) perturbations by quantum fluctuations of the metric tensor. It is usually believed that only scalar modes feed structure formation, while primordial gravitational waves (GWs) contribute to cosmic microwave background (CMB) temperature anisotropies and polarization, while not affecting the large-scale structure (LSS) of the Universe. The only considered exceptions to this rule come from the so-called “tensor fossils,” where large-amplitude long-wavelength GW couple to scalar modes giving rise to specific anisotropic signatures in the LSS [2–4], and from indirect effects of GWs in the LSS clustering and shear [5–7] or galaxy shapes [8].

In this Letter, we explore a novel mechanism for generating matter-density perturbations based upon the nonlinear evolution of primordial tensor modes. This mechanism was first proposed and analyzed in Refs. [9–11]. These tensor-induced scalar modes are statistically independent of standard adiabatic density perturbations, so that the overall matter power spectrum is merely the sum of the ones from the two components. Because of the fact that gravitational waves are frozen on superhorizon scales, they can source our second-order perturbations only on subhorizon scales, so our effect does not produce CMB anisotropies on large scales, unlike the linear matter perturbation. Here we consider scales which entered the Hubble radius after matter-radiation equality. A more

detailed analysis where smaller scales are included will be presented in a separate paper [12].

Our main result is that primordial GWs can lead to observable effects in the matter power spectrum. In particular, we focus here on models of inflation where the linear tensor power spectrum is either blue-tilted or endowed with a Gaussian bump, as it happens, e.g., in axion inflation models [13–15]. Such models, which are also good candidates to be probed by next-generation GW interferometers, such as LISA or ET [16,17], leave an observable imprint on LSS. This opens the possibility to constrain or to detect primordial GWs through future LSS surveys, such as Euclid [18], DESI [19], SPHEREx [20], SKA [21], Roman Space Telescope [22], and Vera Rubin Observatory (LSST) [23].

Tensor-induced scalar modes.—Nowadays, the use of linear perturbation theory (e.g., Refs. [24,25]) is well justified for very large scales and as long as mainly the (matter) power spectrum is considered. On the other hand, higher-order perturbation theory [26–28] (or more sophisticated resummation techniques [29–32]) is needed, as soon as one extends the analysis to higher-order correlators (such as the bispectrum or trispectrum) or aims to describe LSS formation on mildly nonlinear scales and/or in connection with galaxy bias schemes. In this context, one of the main focuses, recently revived, has been the scalar perturbations as seeds of second-order tensor ones, for the obvious reason that they are the dominant ones at linear order. Discussion of scalar-induced gravitational waves can be found in various works, such as Refs. [11,33–43] (see also Ref. [44] for a review).

In this Letter, we present the opposite case; i.e., we look for the signature of GW on cosmic structures.

Detecting the primordial GW background is one of the major goals of cosmology, pursued both through CMB polarization data [45–47] and, after the recent ground-breaking detection of astrophysical GWs [48], also at future interferometers [49–51]. According to the mechanism studied in what follows, GWs produced in the early Universe (see, e.g., Refs. [45,52–54]) can source scalar perturbations upon reentering the horizon [55]. By studying their effect on the matter perturbations, we also aim to provide a new way to constrain the tensor-to-scalar perturbation ratio on scales where we have poor constraints.

In our analysis, we consider a spatially flat Friedmann-Lemaître-Robertson-Walker background metric perturbed up to second order $ds^2 = a^2(\eta)[-d\eta^2 + \gamma_{ij}(\mathbf{x}, \eta)dx^i dx^j]$; here, η is the conformal time and $a(\eta)$ the scale factor. In our analysis, we restrict ourselves to include collisionless cold dark matter plus a cosmological constant; these simplifications allow us to perform our calculations in the synchronous and comoving gauge, which, because of the absence of pressure gradients, can also be made time orthogonal [57]. The conformal spatial metric γ_{ij} contains linear scalar and tensor modes (linear vector modes are not considered here, as they would decay in an expanding universe). At second order, one has scalar-driven scalar, vector, and tensor perturbations, second-order terms mixing linear scalar and tensors (i.e., “tensor fossils,” as mentioned above), tensor-induced vector and tensor modes [11], and finally, the tensor-induced scalar modes, which we are most interested in here (see also Refs. [58,59]). Since the latter are statistically independent of linear scalar modes, we are allowed to deal separately with them, recovering the effect of standard density perturbations at the end. Hence, we take only tensor modes at first order and only scalar ones at second order: $\gamma_{ij} = (1 - \phi^{(2)})\delta_{ij} + (1/2)D_{ij}\chi^{\parallel(2)} + \chi_{ij}^{(1)T}$ where $\chi_{ij}^{(1)T}$ are the linear tensor modes (GW), $D_{ij} = \partial_i \partial_j - (1/3)\nabla^2 \delta_{ij}$, and $\phi^{(2)}$ and $\chi^{\parallel(2)}$ are tensor-induced scalar metric perturbations.

We get the fluid deformation tensor by subtracting the isotropic background expansion from the covariant derivative of the four-velocity $\theta_\nu^\mu = au_{,\nu}^\mu - \mathcal{H}\delta_\nu^\mu$. Choosing comoving observers yields a huge advantage, as it keeps the fluid four-velocity orthogonal to the constant-time spatial hypersurface (described by γ_{ij}), so that our θ_ν^μ is purely spatial, coinciding with the extrinsic curvature of constant-time spatial hypersurfaces $\theta_j^i = -K_j^i = \gamma^{ik}\gamma'_{kj}/2$, with a prime denoting differentiation with respect to conformal time. Our main equations are the Raychaudhuri and continuity equations [11,60]

$$\theta' + \mathcal{H}\theta + \theta_j^i \theta_i^j + 4\pi G a^2 \bar{\rho}_m \delta = 0, \quad (1)$$

$$\delta' + (1 + \delta)\theta = 0, \quad (2)$$

where θ is the peculiar volume expansion scalar, $\mathcal{H} \equiv a'/a$, $\bar{\rho}_m$ the mean energy density of the matter component, and δ its density contrast $\delta = (\rho_m - \bar{\rho}_m)/\bar{\rho}_m$.

We write the density perturbation as $\delta = \delta^{(1)} + \delta^{(2)}/2$, and similarly for θ . Now, from Eqs. (1) and (2) at second order, we get

$$\theta'^{(2)} + \mathcal{H}\theta^{(2)} + 2\theta_j^{(1)i}\theta_i^{(1)j} + 4\pi G a^2 \bar{\rho}_m \delta^{(2)} = 0, \quad (3)$$

$$\delta'^{(2)} + 2\delta^{(1)}\theta^{(1)} + \theta^{(2)} = 0. \quad (4)$$

We combine these to get ($\chi_{ij}^{(1)T} = \chi_{ij}$ from here on)

$$\delta^{(2)''} + \mathcal{H}\delta^{(2)'} - 4\pi G a^2 \bar{\rho}_m \delta^{(2)} = \frac{1}{2}\chi'^{ij}\chi'_{ij}. \quad (5)$$

As expected, the lhs of this equation coincides with the evolution equation for the linear density contrast, but a source term appears, which is quadratic in the tensor perturbation modes. Remembering that the GW energy density is given by $\rho_{\text{GW}} = (1/32\pi G a^2)\langle\chi'^{ij}\chi'_{ij}\rangle$, it is clear that this is the quantity sourcing $\delta^{(2)}$ in Eq. (5).

Density contrast.—The homogeneous and sourced solutions of Eq. (5) are, respectively,

$$\delta_h^{(2)} = c_1(\mathbf{x})D_+(\eta) + c_2(\mathbf{x})D_-(\eta), \quad (6)$$

$$\begin{aligned} \delta_s^{(2)} = & D_+(\eta) \int_0^\eta d\tilde{\eta} \frac{D_-(\tilde{\eta})}{W(\tilde{\eta})} \frac{1}{2}\chi'^{ij}\chi'_{ij} \\ & - D_-(\eta) \int_0^\eta d\tilde{\eta} \frac{D_+(\tilde{\eta})}{W(\tilde{\eta})} \frac{1}{2}\chi'^{ij}\chi'_{ij}, \end{aligned} \quad (7)$$

where D_+ and D_- are the linear growing and decaying homogeneous solutions, and $W(\eta) \equiv D_-(\eta)D'_+(\eta) - D_+(\eta)D'_-(\eta)$ is the Wronskian. From Eq. (7), we can see that our density contrast, though derived at second order, evolves in time just like the linear one.

Here we focus on scalar modes entering the horizon during matter domination (we will include the effects of dark energy later on). In order to compute the power spectrum, we move to Fourier space and write

$$\chi_{ij}(\mathbf{x}, \eta) = \sum_\sigma \int \frac{d^3\mathbf{k}}{(2\pi)^3} e^{i\mathbf{k}\cdot\mathbf{x}} \chi_\sigma(\mathbf{k}, \eta) \epsilon_{ij}^\sigma(\hat{\mathbf{k}}), \quad (8)$$

where $\epsilon_{ij}^\sigma(\hat{\mathbf{k}})$ are the polarization tensors [i.e., $\epsilon_{ij}^\sigma(\hat{\mathbf{k}})\epsilon^{\sigma'ij}(\hat{\mathbf{k}}) = 2\delta_{\sigma\sigma'}$] for the two GW polarizations $\sigma = +, \times$, and $\chi_\sigma(\mathbf{k}, \eta)$ is the GW mode function which sources the scalar perturbations. Having in mind scales which entered the Hubble radius in matter domination, we can make use of the following tensor transfer function [54] $\chi_\sigma(\mathbf{k}, \eta) = A_\sigma(\mathbf{k})[3j_1(k\eta)/k\eta]$, where j_1 is the spherical Bessel function of order one, and $A_\sigma(\mathbf{k})$ is a stochastic

zero-mean random field characterized by the following autocorrelation function:

$$\langle A_{\sigma_1}(\mathbf{k}_1)A_{\sigma_2}(\mathbf{k}_2) \rangle = (2\pi)^3 \delta^3(\mathbf{k}_1 + \mathbf{k}_2) \delta_{\sigma_1\sigma_2} \frac{2\pi^2}{k_1^3} \Delta_\sigma^2(k_1), \quad (9)$$

$\Delta_\sigma^2(k)$ being the power spectrum for each GW polarization.

The time integral in Eq. (7) can be split into two parts, from the end of inflation to matter-radiation equality, and from equality to the observation time. The growing and decaying solutions for density perturbations, as well as the transfer function for the source GWs, should be appropriately chosen for the respective integrals. In the first radiation-dominated part, linear density perturbations involve two modes $D_+ = \ln \eta$ and $D_- = \text{const}$, whereas the GW transfer function behaves as $j_0(k\eta)$, while in the matter era, $D_+ = \eta^2$ and $D_- = \eta^{-3}$, and the GW transfer function is proportional to $j_1(k\eta)$. However, as we will explain later, the contribution from the first part is negligible compared to the second one.

The power spectrum of the stochastic GW background depends on the specific mechanism by which it was generated. In this Letter, we mainly focus on inflationary models which are characterized either by a monochromatic spectrum or by a blue tensor spectrum or by a Gaussian bump. Moreover, we consider parity-invariant mechanisms of production of GWs, so we expect that both polarizations give the same effect, leaving for a future analysis the possibility to consider parity breaking early Universe models.

Power spectrum.—Our final goal is to study the present-day matter power spectrum, taking into account the effect from this tensor-induced perturbation and explore how to infer such an effect from its imprint on the LSS. Following the discussion before, we can evaluate the time integral purely in the matter era, extending the lower limit of time integration down to 0. According to the definition of matter power spectrum $\Delta_\delta^2(k)$,

$$\langle \delta^{(2)}(\mathbf{k}, \eta) \delta^{(2)}(\mathbf{k}', \eta) \rangle = (2\pi)^3 \delta^3(\mathbf{k} + \mathbf{k}') \frac{2\pi^2}{k^3} \Delta_{\delta^{(2)}}^2(k), \quad (10)$$

and using Eq. (9), we get the following expression:

$$\begin{aligned} \Delta_{\delta^{(2)}}^2(k) &= \frac{k^3}{2\pi} \sum_{\sigma, \sigma'} \int d^3\mathbf{k}_2 \frac{\Delta_{\sigma'}^2(k_2) \Delta_\sigma^2(|\mathbf{k} - \mathbf{k}_2|)}{k_2^3 |\mathbf{k} - \mathbf{k}_2|^3} f(k, k_2, \theta) \\ &\times \left[\frac{\eta^2}{10} \int_0^\eta \frac{d\tilde{\eta}}{\tilde{\eta}} \left(\frac{3j_1(k_2\tilde{\eta})}{k_2\tilde{\eta}} \right)' \left(\frac{3j_1(|\mathbf{k} - \mathbf{k}_2|\tilde{\eta})}{|\mathbf{k} - \mathbf{k}_2|\tilde{\eta}} \right)' \right. \\ &\left. - \frac{1}{10\eta^3} \int_0^\eta d\tilde{\eta} \tilde{\eta}^4 \left(\frac{3j_1(k_2\tilde{\eta})}{k_2\tilde{\eta}} \right)' \left(\frac{3j_1(|\mathbf{k} - \mathbf{k}_2|\tilde{\eta})}{|\mathbf{k} - \mathbf{k}_2|\tilde{\eta}} \right)' \right]^2, \end{aligned} \quad (11)$$

where we have defined $f(k, k_2, \theta)$ to be the following contraction of the polarization tensors

$$f(k, k_2, \theta) \equiv \sum_{\sigma, \sigma'} e_{ij}^{\sigma'}(\hat{\mathbf{k}}_2) e^{\sigma ij}(\widehat{\mathbf{k} - \mathbf{k}_2}) e_{kl}^{\sigma'}(-\hat{\mathbf{k}}_2) e^{\sigma kl}(-\widehat{\mathbf{k} + \mathbf{k}_2}).$$

Here, θ is the angle between $\hat{\mathbf{k}}$ and $\hat{\mathbf{k}}_2$. In the convolution and all the expressions from hereon, \mathbf{k} always corresponds to the induced scalar modes, and \mathbf{k}_2 , $(\mathbf{k} - \mathbf{k}_2)$ correspond to the source GW modes. Here, we confine ourselves to the standard practice of dealing with the growing mode only, which we believe to be sufficient. GW modes are frozen outside the horizon, so from Eq. (7), we can see that in Eq. (11) the contribution will come after horizon entry, when GWs start oscillating with an amplitude damped by a factor $\sim 1/a$. As we are considering scalar modes crossing the horizon during matter domination, we can safely switch on our sourcing at $\eta = 0$, since at that early time our modes are superhorizon, and hence are not triggered. Moreover, since after entering the horizon, GWs decay away, and we consider $\eta \rightarrow \infty$ as an upper bound of the time integral instead of putting the exact age of the Universe, as most of the contribution will come from around the time of horizon entry anyway.

To solve such integrals, it is useful to work with the variables $x = k_2/k$, $y = |\mathbf{k} - \mathbf{k}_2|/k$, and use the dimensionless time variable $\tau = k\tilde{\eta}$ [61]. Considering only the growing-mode term in the square brackets of Eq. (11), we get

$$\begin{aligned} \Delta_{\delta^{(2)}}^2(k) &= \frac{81k^4\eta^4}{100} \int_0^\infty dx \int_{|x-1|}^{x+1} dy (xy)^{-2} f(x, y) \Delta_\sigma^2(xk) \Delta_\sigma^2(yk) \\ &\times \left[\int_0^\infty \frac{d\tau}{\tau^3} j_2(x\tau) j_2(y\tau) \right]^2, \end{aligned} \quad (12)$$

where the function f in terms of x and y now reads

$$\begin{aligned} f(x, y) &= \frac{1}{16x^4y^4} [x^8 + (y^2 - 1)^4 + 4x^6(7y^2 - 1) \\ &+ 4x^2(y^2 - 1)^2(7y^2 - 1) + x^4(6 - 60y^2 + 70y^4)]. \end{aligned} \quad (13)$$

There are two important points to stress here: one is the wave-vector integration domain that now, in terms of x and y , is given by [41] $(x + y) \geq 1 \wedge (x + 1) \geq y \wedge (y + 1) \geq x$ and the second is the time integration domain that has been extended to $\eta \rightarrow \infty$ for the reasons explained above. This allows us to solve the integral analytically in terms of hypergeometric functions. We have indeed checked that the contribution from η to infinity is negligible compared to the contribution from 0 to η .

Let us stress here that, although our density contrast modes strictly lie in the matter domination regime, in calculating Eq. (12), we are integrating over the whole frequency range of GW modes, using the appropriate

transfer functions shown in Eq. (11). This is despite the fact that the transfer functions in Eq. (11) are valid only for tensor modes entering the horizon during matter domination. However, we have checked that tensor modes entering during radiation domination constitute a negligible contribution of the resulting signal.

Results for different GW sources.—The spectrum of the GW background depends on the details of the generation mechanism. Besides the standard vacuum oscillations of the gravitational field during inflation, there are many other well-motivated early Universe scenarios which can produce a large GW background also at small scales. Within inflationary mechanisms, this is the case, e.g., of models where the inflaton is coupled to gauge [i.e., U(1) or SU(2)] fields [62,63], or models where space diffeomorphisms are broken during inflation [64–66]. Also, primordial black holes formed via the gravitational collapse of small-scale curvature perturbations, are a powerful source of second-order GWs [42,67]. Regarding postinflationary mechanisms, a strong GW signal can be produced by topological defects [68,69] or phase transitions [70,71]. As we will show in the coming section, all the models that have a large monopole GW signal can source the density perturbation affecting in this way the matter power spectrum.

So, now we are going to quantify the impact on the matter power spectrum (12) for different input GW signals. The power spectrum for individual polarization modes is related to the GW power spectrum by the relation $\Delta_\sigma^2(k) = (1/2)\Delta_T^2(k)$. It is important to stress that, moving away from CMB scales, we have less stringent bounds on the amplitude of the GW spectrum. This allows us to choose larger values for their amplitude.

Power-law spectrum.—As a first benchmark signal, we consider a power-law spectrum, which is typical of many single-field inflationary models [53]

$$\Delta_T^2(k_2) = A_T \left(\frac{k_2}{k_*}\right)^{n_T}. \quad (14)$$

Here, A_T is the amplitude at a given reference or pivot scale k_* , and n_T is the tensor spectral index. Usually A_T is translated in terms of the tensor-to-scalar ratio r defined as the ratio between the tensor and scalar power-spectrum amplitudes at k_* , $r_{k_*} = A_T/A_S$. Standard single-field, slow-roll inflationary models predict a nearly scale-invariant power spectrum on superhorizon scales (with $n_T = -2\epsilon$, with ϵ being the usual slow-roll parameter). On CMB scales, the tensor-to-scalar ratio is strongly constrained by the latest Planck data, $r_{0.01} < 0.066$ (at 95% CL, PLANCK TT, TE, EE + lowE + lensing + BK15 + LIGO & Virgo2016) constraining $-0.76 < n_T < 0.52$ [72]. We consider the case of a blue-tilted tensor power-spectrum, choosing $n_T = 0.32$, which is still within the range of values allowed by present and future GW interferometers [16,72], and fix the GW power-spectrum

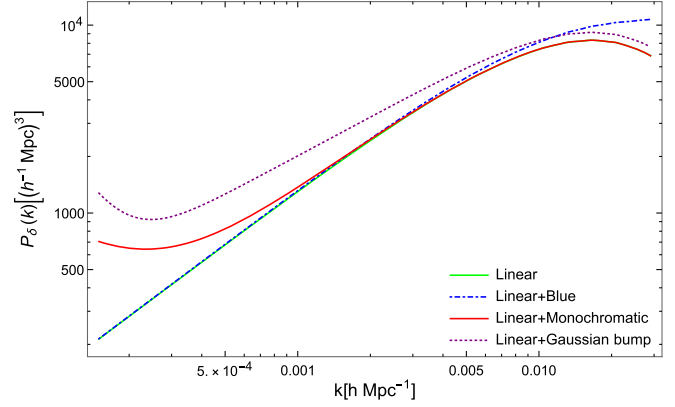


FIG. 1. Impact of different GW power spectra on the matter power spectrum: (i) blue-tilted ($A_T = 1.26 \times 10^{-10}$, $n_T = 0.32$, $k_* = k_{\text{CMB}} = 0.01 \text{ Mpc}^{-1}$), (ii) monochromatic ($A_T = 10^{-5}$, $k_* = 0.008 \text{ Mpc}^{-1}$), and (iii) Gaussian bump ($A_T = 10^{-5}$, $\sigma = 2$, $k_p = 0.04 \text{ Mpc}^{-1}$). The value of h is fixed at 0.68 [73].

amplitude at $A_T = rA_S = 0.06 \times 2.1 \times 10^{-9} = 1.26 \times 10^{-10}$. We can observe in Fig. 1, that the effect starts to be relevant, especially on relatively large k .

Monochromatic spectrum.—A useful case study is a monochromatic tensor spectrum, which can be regarded as an approximation of a spectrum with a sharp peak

$$\Delta_T^2(k_2) = A_T \delta\left(\ln \frac{k_2}{k_*}\right). \quad (15)$$

Typical models that predict such a spectrum can be found in Ref. [74]. In this case, the form of the power spectrum can be found analytically, and it reads

$$\Delta_{\delta^{(2)}}^2(k) = 4 \times 10^{-5} (k\eta_0)^4 A_T^2 \times \left(\frac{8k_*^2}{k^2} + \frac{k^6}{16k_*^6} - \frac{k^4}{2k_*^4} + 3\frac{k^2}{k_*^2} - 8 \right) \Theta(2k_* - k), \quad (16)$$

where the condition $k < 2k_*$ comes from momentum conservation.

Gaussian-bump spectrum.—A well-motivated early Universe scenario which predicts a large and characteristic amplitude for the GW spectrum consists of a GW signal endowed with a large Gaussian bump. An example where we see this kind of bump is an axion field coupled to SU(2) gauge fields as spectator fields besides the inflaton [13,14]. Such models result in GWs which are amplified at the same level as the scalar perturbation, and so they are possible targets both for CMB B -mode observations [14] and interferometers [16,75]. Therefore, for our purposes, one can study their signatures on the matter power spectrum as another way to test or constrain such early Universe scenarios. The tensor power spectrum is characterized by the following Gaussian bump:

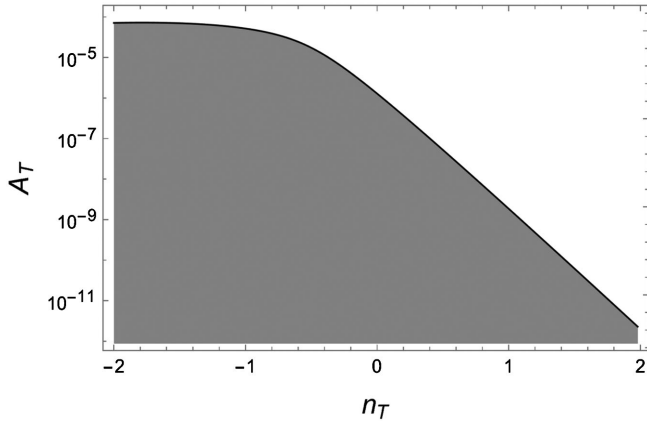


FIG. 2. The region of parameter space for n_T and A_T where the power spectrum of the GW-sourced density perturbation mode with the wave number $k = 0.006 \text{ Mpc}^{-1}$ obeys a 4% error bound on the linear matter power spectrum for a power-law GW source. The gray region shows the allowed range of the parameters assuming the mentioned error uncertainty.

$$\Delta_T^2(k_2) = A_T e^{-\frac{1}{2\sigma^2} \ln^2\left(\frac{k_2}{k_p}\right)}. \quad (17)$$

The impact on the matter power spectrum is visible in Fig. 1, where the effect of the Gaussian bump reflects also on the shape of the matter power spectrum. In Fig. 1, we report the standard matter power spectrum and the one including the effects computed in this Letter. The dimensional power spectrum of matter we show in the plot is related to the dimensionless $\Delta_{\delta^{(2)}}^2(k)$ derived from Eq. (12) through the relation $P_{\delta^{(2)}}(k) = (2\pi^2/k^3)\Delta_{\delta^{(2)}}^2(k)$. Some of these effects are similar or degenerate with other cosmological observable like non-Gaussianity, projection effects, kinetic dipole, finger of the observer, and wide-angle effects (e.g., see Refs. [76–80]), so it is important to find also other peculiar signatures.

We can see that different kinds of GW sources result in extra contributions to the matter power spectrum which are comparable to, and exceeding the linear power spectrum, in different ranges of wave numbers. We calculate Eq. (12) as a function of A_T and n_T for a power-law GW spectrum (14), and considering a 4% error bound with respect to the linear matter power spectrum at $k = 0.006 \text{ Mpc}^{-1}$, we obtain the parameter space shown in Fig. 2. The gray region shows the allowed range for n_T – A_T accounting for the mentioned error.

Including the effect of the dark energy.—All of our analyses so far have been done under the assumption that after matter-radiation equality, the Universe is dominated by cold dark matter only. Choosing an Ω_m different from 1 results in a different linear growth factor D_+ [in Eqs. (6) or (7)], which suppresses the matter growth. The fitting formula for the growth suppression factor for linear density perturbation is given in Refs. [81,82]. Using $\Omega_m = 0.32$ [73], we find our suppressed power spectrum to be

$P_{\delta^{(2)}}(z=0, \Omega_m=0.32) \simeq 0.59 P_{\delta^{(2)}}(z=0, \Omega_m=1)$. Figure 1 already includes the dark energy component.

Early-time evolution.—In the previous sections, we have discussed the induced matter perturbation modes entering the horizon during matter domination. As anticipated, the contribution from the modes which enter before matter-radiation equality is negligible compared to the former one. Here, we briefly discuss what we may have to face in the era when radiation was the dominant component. Second-order perturbations in synchronous gauge for the scalar-tensor and tensor-tensor couplings are discussed in Refs. [58] and [83], respectively, for the matter- and radiation-dominated stages, although their full matter power spectra were not studied.

At early times, the Universe consists of a mixture of radiation and pressureless matter. Since there are two matter components now, we would not have the advantage of having the fluid four-velocity tensor orthogonal to the spatial hypersurface anymore. Instead, we have to use the conservation equations for both components and the Einstein equations. Since the radiation and cold dark matter components interact only gravitationally, their energy-momentum tensors satisfy their conservation laws separately. The standard way of dealing with this scenario is to consider two phases: first, very early times when the gravitational potential is solely determined by radiation and determines matter perturbations, and second, when the matter perturbation grows significantly toward the equality time and dominantly contributes to the potential. In this case, we would get the Meszaros’s equation for the subhorizon evolution of matter perturbation in a universe filled with radiation and matter [84–87], but now with a source term. In order to know the full nonlinear evolution at second order, we then need to solve the inhomogeneous equation. This is a treatment we leave for a future work.

Discussion and conclusion.—In this Letter, we have analyzed the new effect of “tensor-induced scalar modes” on the present-day matter power spectrum. We have found that a large GW power spectrum can leave an imprint on the matter power spectrum. There are two important features of our second-order matter perturbation: First, we do not have a contribution on superhorizon scales, unlike the linear matter perturbation, and as a result, our effect does not produce CMB temperature anisotropy on large scales. Second, our matter density contrast completely mimics the linear one on the subhorizon scales. In that sense, it can be considered as a linear perturbation sourced by gravitational radiation vanishing outside the horizon. A distinguishing feature would be its high intrinsic non-Gaussianity, which we intend to explore in the future. We have also showed the parameter space for the tensor spectral index versus the GW amplitude, accounting for the uncertainties on the measurements of the matter power spectrum. This signature can be useful both for detecting and constraining GWs in a novel way on a range of scales on which we currently have very poor

information and to increase the accuracy in the estimation of matter power spectrum.

P. B. and S. M. sincerely thank Serena Giardiello for her help in clarifying some concepts. A. R. thanks Stefano Anselmi, Mauro Pieroni, and Lorenzo Valbusa Dall'Armi for useful comments and discussions. N. B., D. B. and S. M. acknowledge support from the COSMOS network through the ASI (Italian Space Agency) Grants No. 2016-24-H.0 and No. 2016-24-H.1-2018. A. R. and P. B. acknowledge funding from Italian Ministry of Education, University and Research through the "Dipartimenti di eccellenza" project Science of the Universe.

*pbari@pd.infn.it

†angelo.ricciardone@pd.infn.it

‡nicola.bartolo@pd.infn.it

§daniele.bertacca@pd.infn.it

||sabino.matarrese@pd.infn.it

- [1] A. H. Guth, The inflationary universe: A possible solution to the horizon and flatness problems, *Phys. Rev. D* **23**, 347 (1981).
- [2] K. W. Masui and U.-L. Pen, Primordial Gravity Wave Fossils and Their Use in Testing Inflation, *Phys. Rev. Lett.* **105**, 161302 (2010).
- [3] D. Jeong and M. Kamionkowski, Clustering Fossils from the Early Universe, *Phys. Rev. Lett.* **108**, 251301 (2012).
- [4] E. Dimastrogiovanni, M. Fasiello, D. Jeong, and M. Kamionkowski, Inflationary tensor fossils in large-scale structure, *J. Cosmol. Astropart. Phys.* **12** (2014) 050.
- [5] N. Kaiser and A. H. Jaffe, Bending of light by gravity waves, *Astrophys. J.* **484**, 545 (1997).
- [6] D. Jeong and F. Schmidt, Large-scale structure with gravitational waves I: Galaxy clustering, *Phys. Rev. D* **86**, 083512 (2012).
- [7] F. Schmidt and D. Jeong, Large-scale structure with gravitational waves II: Shear, *Phys. Rev. D* **86**, 083513 (2012).
- [8] M. Biagetti and G. Orlando, Primordial gravitational waves from galaxy intrinsic alignments, *J. Cosmol. Astropart. Phys.* **07** (2020) 005.
- [9] K. Tomita, Non-linear theory of gravitational instability in the expanding universe. II, *Prog. Theor. Phys.* **45**, 1747 (1971).
- [10] K. Tomita, Non-linear theory of gravitational instability in the expanding universe. III, *Prog. Theor. Phys.* **47**, 416 (1972).
- [11] S. Matarrese, S. Mollerach, and M. Bruni, Second order perturbations of the Einstein–de Sitter universe, *Phys. Rev. D* **58**, 043504 (1998).
- [12] P. Bari *et al.* (to be published).
- [13] R. Namba, M. Peloso, M. Shiraishi, L. Sorbo, and C. Unal, Scale-dependent gravitational waves from a rolling axion, *J. Cosmol. Astropart. Phys.* **01** (2016) 041.
- [14] B. Thorne, T. Fujita, M. Hazumi, N. Katayama, E. Komatsu, and M. Shiraishi, Finding the chiral gravitational wave background of an axion-SU(2) inflationary model using CMB observations and laser interferometers, *Phys. Rev. D* **97**, 043506 (2018).
- [15] E. Dimastrogiovanni, M. Fasiello, and T. Fujita, Primordial gravitational waves from axion-gauge fields dynamics, *J. Cosmol. Astropart. Phys.* **01** (2017) 019.
- [16] N. Bartolo *et al.*, Science with the space-based interferometer LISA. IV: Probing inflation with gravitational waves, *J. Cosmol. Astropart. Phys.* **12** (2016) 026.
- [17] M. Maggiore *et al.*, Science case for the Einstein Telescope, *J. Cosmol. Astropart. Phys.* **03** (2020) 050.
- [18] A. Blanchard *et al.*, Euclid preparation: VII. Forecast validation for Euclid cosmological probes, *Astron. Astrophys.* **642**, A191 (2020).
- [19] A. Dey *et al.*, Overview of the DESI Legacy Imaging Surveys, *Astron. J.* **157**, 168 (2019).
- [20] O. Doré *et al.*, Science impacts of the SPHEREx all-sky optical to near-infrared spectral survey: Report of a community workshop examining extragalactic, galactic, stellar and planetary science, [arXiv:1606.07039](https://arxiv.org/abs/1606.07039).
- [21] D. J. Bacon *et al.*, Cosmology with phase 1 of the square kilometre array: Red book 2018: Technical specifications and performance forecasts, *Pub. Astron. Soc. Aust.* **37**, e007 (2020).
- [22] B. M. Rose *et al.*, A reference survey for supernova cosmology with the Nancy Grace Roman Space Telescope, [arXiv:2111.03081](https://arxiv.org/abs/2111.03081).
- [23] R. L. Jones *et al.* (Vera C. Rubin Observatory LSST Solar System Science Collaboration), The scientific impact of the Vera C. Rubin Observatory's Legacy Survey of Space and Time (LSST) for Solar System science, [arXiv:2009.07653](https://arxiv.org/abs/2009.07653).
- [24] V. F. Mukhanov, H. A. Feldman, and R. H. Brandenberger, Theory of cosmological perturbations. Part 1. Classical perturbations. Part 2. Quantum theory of perturbations. Part 3. Extensions, *Phys. Rep.* **215**, 203 (1992).
- [25] V. Mukhanov, *Physical Foundations of Cosmology* (Cambridge University Press, Cambridge, England, 2005).
- [26] S. Matarrese, O. Pantano, and D. Saez, A general relativistic approach to the nonlinear evolution of collisionless matter, *Phys. Rev. D* **47**, 1311 (1993).
- [27] S. Matarrese, O. Pantano, and D. Saez, General Relativistic Dynamics of Irrotational Dust: Cosmological Implications, *Phys. Rev. Lett.* **72**, 320 (1994).
- [28] C. Döring, S. Centelles Chuliá, M. Lindner, B. M. Schaefer, and M. Bartelmann, Gravitational wave induced baryon acoustic oscillations, *SciPost Phys.* **12**, 114 (2022).
- [29] S. Matarrese and M. Pietroni, Resumming cosmic perturbations, *J. Cosmol. Astropart. Phys.* **06** (2007) 026.
- [30] T. Matsubara, Resumming cosmological perturbations via the Lagrangian picture: One-loop results in real space and in redshift space, *Phys. Rev. D* **77**, 063530 (2008).
- [31] L. Senatore and M. Zaldarriaga, The IR-resummed effective field theory of large scale structures, *J. Cosmol. Astropart. Phys.* **02** (2015) 013.
- [32] Z. Vlah, U. Seljak, M. Y. Chu, and Y. Feng, Perturbation theory, effective field theory, and oscillations in the power spectrum, *J. Cosmol. Astropart. Phys.* **03** (2016) 057.
- [33] S. Matarrese and S. Mollerach, The stochastic gravitational wave background produced by nonlinear cosmological perturbations, in *Proceedings of the "Spanish Relativity Meeting '96", Valencia, Spain, 1996*, edited by J. A. Miralles, J. A. Morales, and D. Saez (1997), p. 87.

- [34] S. Mollerach, D. Harari, and S. Matarrese, CMB polarization from secondary vector and tensor modes, *Phys. Rev. D* **69**, 063002 (2004).
- [35] D. Baumann, P. J. Steinhardt, K. Takahashi, and K. Ichiki, Gravitational wave spectrum induced by primordial scalar perturbations, *Phys. Rev. D* **76**, 084019 (2007).
- [36] K. Inomata and T. Terada, Gauge independence of induced gravitational waves, *Phys. Rev. D* **101**, 023523 (2020).
- [37] C. Yuan, Z.-C. Chen, and Q.-G. Huang, Scalar induced gravitational waves in different gauges, *Phys. Rev. D* **101**, 063018 (2020).
- [38] K. N. Ananda, C. Clarkson, and D. Wands, The cosmological gravitational wave background from primordial density perturbations, *Phys. Rev. D* **75**, 123518 (2007).
- [39] K. Kohri and T. Terada, Semianalytic calculation of gravitational wave spectrum nonlinearly induced from primordial curvature perturbations, *Phys. Rev. D* **97**, 123532 (2018).
- [40] G. Domènech, S. Pi, and M. Sasaki, Induced gravitational waves as a probe of thermal history of the Universe, *J. Cosmol. Astropart. Phys.* **08** (2020) 017.
- [41] J. R. Espinosa, D. Racco, and A. Riotto, A cosmological signature of the SM Higgs instability: Gravitational waves, *J. Cosmol. Astropart. Phys.* **09** (2018) 012.
- [42] R. Saito and J. Yokoyama, Gravitational Wave Background as a Probe of the Primordial Black Hole Abundance, *Phys. Rev. Lett.* **102**, 161101 (2009); **107**, 069901(E) (2011).
- [43] J.-O. Gong, Analytic integral solutions for induced gravitational waves, *Astrophys. J.* **925**, 102 (2022).
- [44] G. Domènech, Scalar induced gravitational waves review, *Universe* **7**, 398 (2021).
- [45] P. A. R. Ade *et al.* (Keck Array and BICEP2 Collaborations), Constraints on Primordial Gravitational Waves Using *Planck*, WMAP, and New BICEP2/Keck Observations through the 2015 Season, *Phys. Rev. Lett.* **121**, 221301 (2018).
- [46] M. Hazumi *et al.*, LiteBIRD: JAXA's new strategic L-class mission for all-sky surveys of cosmic microwave background polarization, *Proc. SPIE Int. Soc. Opt. Eng.* **11443**, 114432F (2020).
- [47] K. Abazajian *et al.* (CMB-S4 Collaboration), CMB-S4: Forecasting constraints on primordial gravitational waves, *Astrophys. J.* **926**, 54 (2022).
- [48] B. P. Abbott *et al.*, Observation of Gravitational Waves from a Binary Black Hole Merger, *Phys. Rev. Lett.* **116**, 061102 (2016).
- [49] C. Caprini, D. G. Figueroa, R. Flauger, G. Nardini, M. Peloso, M. Pieroni, A. Ricciardone, and G. Tasinato, Reconstructing the spectral shape of a stochastic gravitational wave background with LISA, *J. Cosmol. Astropart. Phys.* **11** (2019) 017.
- [50] P. Campeti, E. Komatsu, D. Poletti, and C. Baccigalupi, Measuring the spectrum of primordial gravitational waves with CMB, PTA and laser interferometers, *J. Cosmol. Astropart. Phys.* **01** (2021) 012.
- [51] R. Flauger, N. Karnesis, G. Nardini, M. Pieroni, A. Ricciardone, and J. Torrado, Improved reconstruction of a stochastic gravitational wave background with LISA, *J. Cosmol. Astropart. Phys.* **01** (2021) 059.
- [52] M. Maggiore, Gravitational wave experiments and early Universe cosmology, *Phys. Rep.* **331**, 283 (2000).
- [53] M. C. Guzzetti, N. Bartolo, M. Liguori, and S. Matarrese, Gravitational waves from inflation, *Riv. Nuovo Cimento* **39**, 399 (2016).
- [54] Y. Watanabe and E. Komatsu, Improved calculation of the primordial gravitational wave spectrum in the standard model, *Phys. Rev. D* **73**, 123515 (2006).
- [55] An analogous effect was found in Ref. [56], where second-order density perturbations arising from quantum fluctuations of electromagnetic waves were analyzed.
- [56] C.-H. Wu, K.-W. Ng, and L. H. Ford, Possible constraints on the duration of inflationary expansion from quantum stress tensor fluctuations, *Phys. Rev. D* **75**, 103502 (2007).
- [57] H. Kodama and M. Sasaki, Cosmological perturbation theory, *Prog. Theor. Phys. Suppl.* **78**, 1 (1984).
- [58] Y. Zhang, F. Qin, and B. Wang, Second-order cosmological perturbations. II. Produced by scalar-tensor and tensor-tensor couplings, *Phys. Rev. D* **96**, 103523 (2017).
- [59] P. Carrilho and K. A. Malik, Vector and tensor contributions to the curvature perturbation at second order, *J. Cosmol. Astropart. Phys.* **02** (2016) 021.
- [60] M. Bruni, J. C. Hidalgo, N. Meures, and D. Wands, Non-Gaussian initial conditions in Λ CDM: Newtonian, relativistic, and primordial contributions, *Astrophys. J.* **785**, 2 (2014).
- [61] N. Bartolo, S. Matarrese, A. Riotto, and A. Vaihkonen, The maximal amount of gravitational waves in the curvaton scenario, *Phys. Rev. D* **76**, 061302(R) (2007).
- [62] N. Barnaby and M. Peloso, Large Non-Gaussianity in Axion Inflation, *Phys. Rev. Lett.* **106**, 181301 (2011).
- [63] L. Sorbo, Parity violation in the cosmic microwave background from a pseudoscalar inflaton, *J. Cosmol. Astropart. Phys.* **06** (2011) 003.
- [64] S. Endlich, A. Nicolis, and J. Wang, Solid inflation, *J. Cosmol. Astropart. Phys.* **10** (2013) 011.
- [65] N. Bartolo, D. Cannone, A. Ricciardone, and G. Tasinato, Distinctive signatures of space-time diffeomorphism breaking in EFT of inflation, *J. Cosmol. Astropart. Phys.* **03** (2016) 044.
- [66] A. Ricciardone and G. Tasinato, Primordial gravitational waves in supersolid inflation, *Phys. Rev. D* **96**, 023508 (2017).
- [67] N. Bartolo, V. De Luca, G. Franciolini, A. Lewis, M. Peloso, and A. Riotto, Primordial Black Hole Dark Matter: LISA Serendipity, *Phys. Rev. Lett.* **122**, 211301 (2019).
- [68] A. Vilenkin, Gravitational radiation from cosmic strings, *Phys. Lett.* **107B**, 47 (1981).
- [69] D. G. Figueroa, M. Hindmarsh, and J. Urrestilla, Exact Scale-Invariant Background of Gravitational Waves from Cosmic Defects, *Phys. Rev. Lett.* **110**, 101302 (2013).
- [70] A. Kosowsky, M. S. Turner, and R. Watkins, Gravitational radiation from colliding vacuum bubbles, *Phys. Rev. D* **45**, 4514 (1992).
- [71] M. Kamionkowski, A. Kosowsky, and M. S. Turner, Gravitational radiation from first order phase transitions, *Phys. Rev. D* **49**, 2837 (1994).
- [72] Y. Akrami *et al.*, Planck 2018 results. X. Constraints on inflation, *Astron. Astrophys.* **641**, A10 (2020).
- [73] N. Aghanim *et al.*, Planck 2018 results. VI. Cosmological parameters, *Astron. Astrophys.* **641**, A6 (2020).

- [74] Y.-F. Cai, C. Lin, B. Wang, and S.-F. Yan, Sound Speed Resonance of the Stochastic Gravitational Wave Background, *Phys. Rev. Lett.* **126**, 071303 (2021).
- [75] J. Garcia-Bellido, M. Peloso, and C. Unal, Gravitational waves at interferometer scales and primordial black holes in axion inflation, *J. Cosmol. Astropart. Phys.* **12** (2016) 031.
- [76] D. Jeong, F. Schmidt, and C. M. Hirata, Large-scale clustering of galaxies in general relativity, *Phys. Rev. D* **85**, 023504 (2012).
- [77] A. Raccanelli, D. Bertacca, D. Jeong, M. C. Neyrinck, and A. S. Szalay, Doppler term in the galaxy two-point correlation function: Wide-angle, velocity, Doppler lensing and cosmic acceleration effects, *Phys. Dark Universe* **19**, 109 (2018).
- [78] L. R. Abramo and D. Bertacca, Disentangling the effects of Doppler velocity and primordial non-Gaussianity in galaxy power spectra, *Phys. Rev. D* **96**, 123535 (2017).
- [79] B. Bahr-Kalus, D. Bertacca, L. Verde, and A. Heavens, The Kaiser-Rocket effect: Three decades and counting, *J. Cosmol. Astropart. Phys.* **11** (2021) 027.
- [80] M. Yousry Elkhatab, C. Porciani, and D. Bertacca, The large-scale monopole of the power spectrum in a Euclid-like survey: Wide-angle effects, lensing, and the “finger of the observer”, *Mon. Not. R. Astron. Soc.* **509**, 1626 (2021).
- [81] J. A. Peacock, *Cosmological Physics* (Cambridge University Press, Cambridge, England, 2010).
- [82] S. M. Carroll, W. H. Press, and E. L. Turner, The cosmological constant., *Annu. Rev. Astron. Astrophys.* **30**, 499 (1992).
- [83] B. Wang and Y. Zhang, Second-order cosmological perturbations IV. Produced by scalar-tensor and tensor-tensor couplings during the radiation dominated stage, *Phys. Rev. D* **99**, 123008 (2019).
- [84] S. Dodelson, *Modern Cosmology* (Academic Press, London, 2021).
- [85] W. Hu and N. Sugiyama, Small scale cosmological perturbations: An analytic approach, *Astrophys. J.* **471**, 542 (1996).
- [86] P. Meszaros, The behaviour of point masses in an expanding cosmological substratum, *Astron. Astrophys.* **37**, 225 (1974).
- [87] E. J. Groth and P. J. E. Peebles, Closed-form solutions for the evolution of density perturbations in some cosmological models, *Astron. Astrophys.* **41**, 143 (1975).